Factors influencing transit fatigue of seamless pipes

H. G. KUNERT and J. L. OTEGUI

University of Mar del Plata, J. B. Justo 4302, 7600 Mar del Plata, Argentina

Received in final form 20 December 2004

ABSTRACT Full-scale fatigue tests simulating real pipe stock conditions in ships were carried out in order to reproduce failures of seamless pipes due to fatigue crack growth during shipping. Simple mechanical analyses were then used to assess the factors that influence transit fatigue. As seen in several actual failures, fatigue cracks were found to propagate from both sides of the pipe wall. It is possible to have transit fatigue (TF) when piling up a few pipes for transportation, if there is previous plastic indentation. Susceptibility to TF was found to be independent of the nature of discontinuities in the surfaces of the pipes. Precautions to reduce the probability of TF in sea shipment include preventing plastic indentation of the pipes and storing stiffer pipes in the bottom part of the hold.

Keywords experiment; seamless piping; shipment; transit fatigue.

INTRODUCTION

This work is a part of a programme to understand the characteristics of transit fatigue (TF). As early as in the mid 1960s fatigue cracks during shipment from the mill were found to produce leaks and breaks during the hydrotest after the construction of the pipeline.[1] The effect of mechanical damage on fracture initiation in line pipe and the resistance of pipelines to mechanical damage have been thoroughly studied.[2–6] It is well known that planar defects within a dent can have an extremely detrimental effect on pipeline reliability.[7] This effect is related both to material degradation and to the stress concentration produced by the defects. These studies, however, refer to TF in larger diameter pipes with longitudinal seams, welded either with submerged arc (SAW) or electrical resistance (ERW) weld procedures. Larger diameter to thickness (D/t) ratio makes these pipes more susceptible to sustain large bending stresses during shipping. The mechanical, metallurgical and geometric discontinuities at the seam weld also contribute to initiate fatigue cracks.

However, recent evidence shows that TF related cracks have indeed been the cause of failures in seamless pipes during preoperational hydrostatic testing or in service.[6] Two cracking patterns have been detected: one is concentric, generates the appearance of 'holes' due to material detachment; and the other is longitudinal, with cracks that begin from both surfaces of the wall of the pipe. The most critical in service failures were due to the propagation of longitudinal cracks. This second crack type can lead to the collapse of the ligament when the pipe is subjected to internal pressure, if the flaw is not detected before the pipe enters in service. Fractographic analyses after the reported failures indicate that the cracking mechanism is related to low cycle, high amplitude fatigue. They present multiple crack initiation from both surfaces, and at the moment of failure or detection the through-the-thickness fracture presented a percentile relationship of around 70/30, with predominance from the outer surface.

A typical example from earlier work by the authors is seen in Fig. 1. In this case, load amplitudes varied and beach marks allow propagation paths of several cracks initiated in both surfaces to follow. No previous defects were identified in either surface. It is reasonable to assume that in order to reproduce this type of cracking tensile stress amplitudes above the fatigue limit for the material are required in both surfaces of the pipe wall. This particular fatigue failure followed a previous plastic indentation at a larger load. These conditions can be obtained when a sudden movement of the cargo in a ship makes a pipe impact on a hard surface at some time during a trip. Bouncing of the ship due to the waves during the trip seems to be effective in initiating and growing fatigue cracks in the indented area. Up to now, it was not clear whether or not previous defects in the material surfaces are necessary to promote TF. Similarly, no outstanding evidence was produced as to whether material embrittlement by plastic deformation is a major factor in the occurrence of

Correspondence: J. L. Otegui. E-mail: jotegui@fi.mdp.edu.ar

Fig. 1 Typical fracture surface due to transit fatigue (TF) in a seamless pipe.

the failures. Because the cracking mechanism is associated with mechanical fatigue, the susceptibility of a certain pipe could strongly depend on its surface finish and its yield strength.

This article discusses the influence of the loads possibly generated during the transportation of seamless pipes by ship and the likelihood of initiation of cracks. Seamless steel pipes of the type API N80[8] were experimentally tested. These pipes are relatively thick and of a small diameter, intended to be used in the oil industry with the general description of oil country tubular goods (OCTG). The main aspects evaluated in this paper are the storage conditions that result in the reported failures. The influence of surface conditions and minor microstructural changes in the pipe material are also assessed.

The experimental crack initiation and propagation data presented in this paper are intended to verify the real nature of fatigue cracks produced during transportation of seamless pipes. Unlike most in service cyclic stresses, which are due to inherent discontinuous or alternating loads, cyclic stresses during transportation can be readily reduced below fatigue threshold. Therefore, rather than attempting a fatigue life prediction, this paper addresses those mechanical aspects that are found to be most effective in increasing the risk for TF failures. Several geometries for hard surfaces indenting the pipes were tested with different load and restraint conditions. The most effective within the subset of those likely to be found in real shipping were analysed in some detail.

In order to assess the incidence of loading and material properties in the TF process of OCTG, two API 5CT N80, 180 mm inner diameter, 9-mm-thick pipes were tested in the laboratory to simulate the conditions of TF. One of the pipes was quenched and tempered (QT), while the other was normalized (OLN).

Fig. 2 Storage of pipes during shipping. (a) typical lateral protection by wood sticks, (b) common hits during loading.

CRITICAL REVIEW OF STOWAGE METHODS IN SHIPS

The holds (or cellars) of several cargo ships were inspected during the stowage of seamless pipes to analyse real possible indenters and methodologies applied to protect the pipes. Figure 2a summarizes a typical stock of seamless

(b)

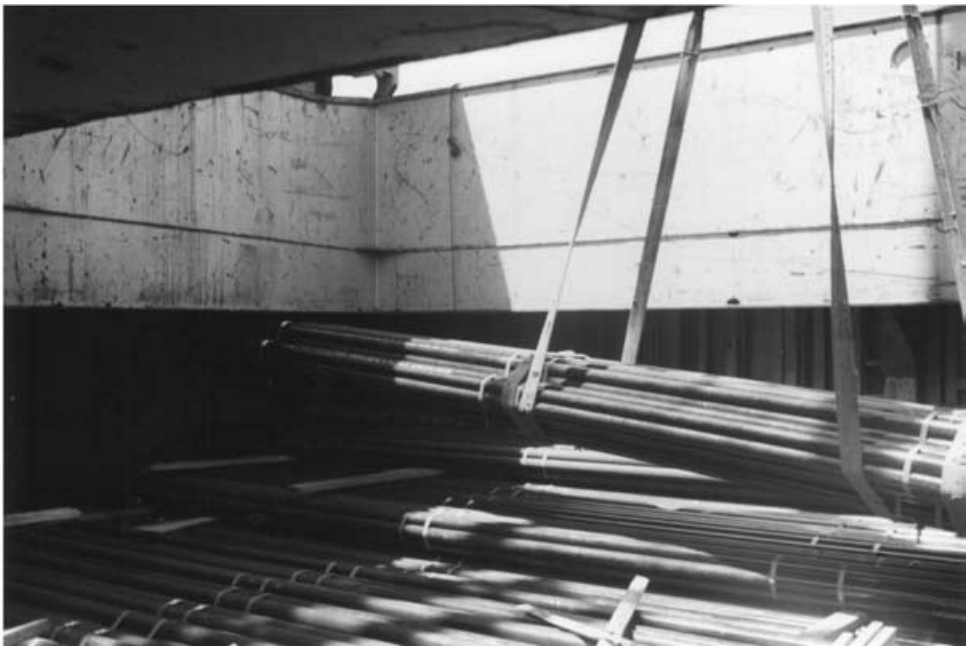

Fig. 2 Continued

pipes during shipping. As seen in this example, due to the delivery sequence, sometimes the longer pipes are stowed above the shorter ones, in which case the long ones are subjected to bending. In most of the places where protuberances create a danger of indentation, wooden piles and batons for protection were appropriately positioned (Fig. 2a). Sometimes, however, the displacement of protecting wood batons leads to stowed pipes being supported against the metallic columns of the holds. Size (length or diameter) of the possible indenters in a typical cargo bay is between 10 mm and 300 mm.

During the stowage manoeuvres, the packages of pipes frequently hit against the gates or hatches (Fig. 2b) causing indentations in the pipes or in the plastic protection of the threaded ends. Steel hand tools used to position the pipes once in the hold are sometimes forgotten and left among the pipes, thus becoming possible indenters. Scratches and other marks found in the holds show that several prominent parts were subjected to blows, probably due to impact against the cargo.

Safety standards used by the inspectors help to avoid accidents during transport, but to a much lesser extent to avoid damage to the pipes. Other heavy products are sometimes stowed on top of the pipes, thus becoming further sources of indentation. During heavy storms sometimes the load suffers massive damages due to movement inside the holds. The height of most of the inspected holds is about 3 m, which allows storage of up to 15 lines of loose pipes, or between 6 and 8 packages, depending on the size and diameter. Some ships have holds up to 20 m high, which allows to store many pipes. In these cases, the dynamic forces on the lower rows of pipes can become large enough to justify the indentations and cracking observed in this and other studies of TF failures in seamless pipes.

MATERIALS CHARACTERIZATION

Tensile test results for both N80 materials are shown in Table 1. The manufacturing residual stresses (S_{res}) were measured in both pipes, and are also shown in Table 1. These are hoop stresses, and were defined by making longitudinal cuts in rings of the pipes and measuring the perimetral separation of both cut edges. Using the usual analytical formulae,[9] it was verified that these stresses have mostly a bending distribution through the wall of the pipes.

Dynamic tests introducing a controlled plastic indentation were carried out to study the influence of the deformation rate on the elastic–plastic behaviour and the toughness of the materials. The impact rate was 5 m/s, which is approximately equivalent to the following hypothetical cases:

- impact by a tractor or similar vehicle at 20 km/h,
- fall of the pipe from a height of 4 m and
- maximum tangential speed of the pendulous movement of the pipes when raised during the stowing manoeuvres in ships (Fig. 2b).

An indentation force of 18 ton was applied by a hydraulic press. Two test conditions were analysed: without lateral

Table 1 Material properties

Pipe	Hoop residual stress S_{res} (MPa)	Lower yield strength S_{yield}^{sup} (MPa)	Upper yield strength S_{yield}^{sup} (MPa)	Ultimate tensile strength S_{uts} (MPa)
N80 N	183.4	624	668.8	820.5
N80 Q and T	208.9	703.3	737.7	772.2
API 5CT	–	551.6	758.4	689.5

restraint, and with a lateral contraction of 1 mm produced by a rigid device. No microcracks were found in the pipes. It was concluded that for the range of deformation rates studied, the materials do not present susceptibility to cracking due to dynamic plastic indentation.

Fatigue crack initiation *S–N* curves were experimentally determined for both materials. These associate the amplitude of the cyclic applied stress state (*S*) with the number of cycles until the detection of cracks (*N*).[10] The methods of linear elastic fracture mechanics (LEFM) were used to assess fatigue crack propagation properties of each material, the applied cyclic stress intensity factor (ΔK) was related to crack propagation rate per cycle ($\mathrm{d}a/\mathrm{d}n$). The simple Paris–Erdogan model was used:

$$\mathrm{d}a/\mathrm{d}n = C\Delta K^m,$$

where C and m are material constants.[10,11] Below a certain threshold value ΔK_o, the cracks are considered to remain inactive. ΔK responds to a general form of the type:

$$\Delta K = Y\sigma\sqrt{\pi a},$$

where σ is the applied stress, a is the crack depth and Y is a factor that depends on the geometry.[12]

A soft (load-controlled) walking beam type mechanical machine was used to characterize fatigue crack initiation and the propagation in three-point bending tests of OLN and QT samples. Three initiation and two propagation tests were carried out for each material, with load amplitudes between 5000 and 8000 N. Fatigue cracks were initiated from the as-manufactured inner surface of the pipes. For the crack propagation tests, longitudinal semi-elliptic notches were machined in the specimens. Crack propagation was monitored using the crack mouth strain gauge technique.[13] The specimens were subjected to cyclic loading, until cracks initiated from the notches. Once these cracks were well developed, $\mathrm{d}a/\mathrm{d}n$ and ΔK measurements were carried out. Marks in the fracture surfaces were introduced during the tests, using beach marking and ink staining, to verify the evolution of crack geometry. The values of ΔK for different positions in the crack front were obtained applying the Newman–Raju equations.[14]

Crack initiation results are shown in Fig. 3a, with the stress state normalized with respect to the yield stress. For a given normalized stress level, initiation lives for the QT material are twice the OLN material. Literature results for QT and ferritic–pearlitic steels confirm a linear relationship between fatigue limit and yield strength.[10] This relationship is linked to the resistance to the formation of

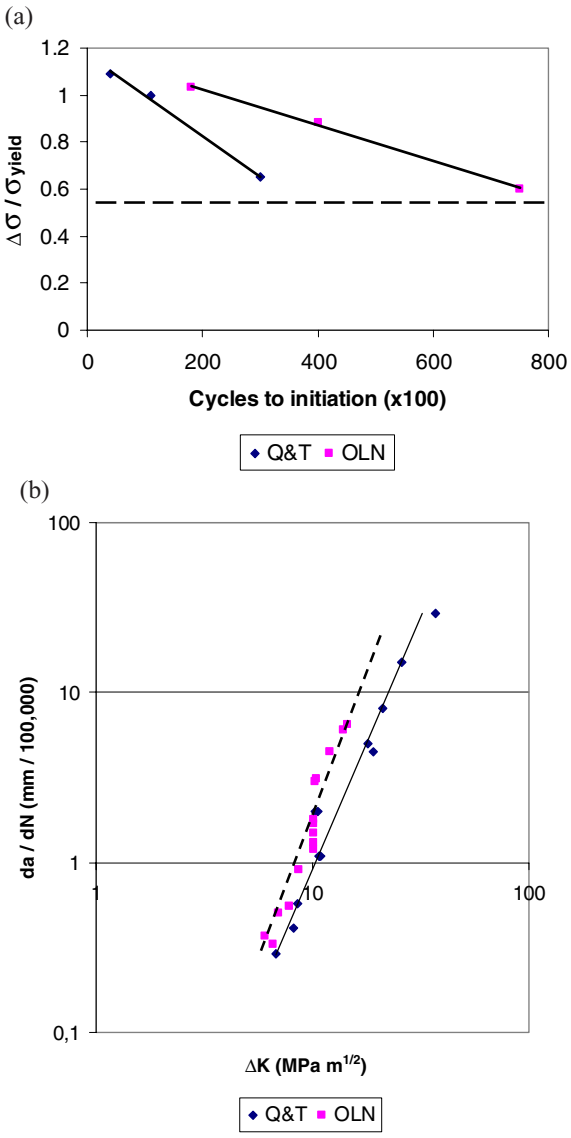

Fig. 3 Fatigue characterization of API 5CT 80 materials. (a) fatigue initiation *S–N* curves, (b) fatigue crack growth rates.

persistent slip bands (PSBs), which is the most common initiation mechanism in the absence of sharp notches or other defects. Fatigue crack growth rates for both materials are shown in Fig. 3b. Propagation rates in the QT are 30% lower than in the OLN.

SIMPLIFIED MODELS OF STRESS STATES DURING TRANSIT FATIGUE

When a pipe is subjected to inner pressure, the circumferential stress is at least twice as high as the longitudinal stress. Therefore, the most dangerous crack pattern is defined by the presence of longitudinal cracks. Evidence from actual TF failures indicate that developed cracks usually arise from both surfaces of the pipe, and both surface cracks propagate to at least 30% wall thickness. In order to identify the stress components required for this crack pattern, first consider the simple model shown in Fig. 4. A vertical load P on a section of a horizontal pipe causes a radial deformation.[9]

$$W = 0.296PR^3/E\mathcal{J},$$

where R and $\mathcal{J}$ are the radius and the moment of inertia of the pipe, and E is the Young modulus of the steel. The maximum traction stress S_e on the outer surface in the horizontal position is

$$Se = 0.637RbP/(2\mathcal{J}),$$

where b is the pipe thickness. The minimum cyclic stress ΔS that would allow fatigue to occur from the outer surface in the absence of defects (Fig. 3a) is close to the fatigue limit, which is about half of the material yield stress S_y.[10] Considering only the effect of the vertical loads, for our pipe dimensions ($R_2 = 90$ mm, $b = 9$ mm) this stress corresponds to a vertical displacement $W = 0.98$ mm.

To simulate the effect of an indenter under elastic conditions, consider now a pipe subjected to a load P concentrated on a small length $2b$ (Fig. 5). This model assumes a load evenly distributed lengthwise, and does not include any shear or friction with the indenter. This load generates longitudinal and circumferential stresses due to local bending of the pipe wall. The maximum traction stresses are located at the midpoint A. The equations for these stresses[9] predict that the circumferential stress state is the sum of a compressive membrane (S_{cm}) and a bending (S_{cb}) component, as shown in Fig. 6.

Positive stress cycles in both surfaces of the pipe can be produced by lateral constraint against adjacent pipes in the stack (above as well as alongside). If no lateral restraint is applied, cracks would initiate from only one side of the pipe. We can assume that the indenter is any unprotected metallic part of the container. The cyclic loads acting laterally when the pipe is subjected to the action of the indenter can be estimated similarly to the dynamic vertical load due to the weight of the pipes. The magnitude of the cyclic load is defined by the portion of the total lateral load acting on the pipe that is transmitted by the indenter. This portion is in turn a function of the distance between the indenter and the other lateral supports, the rigidity of the

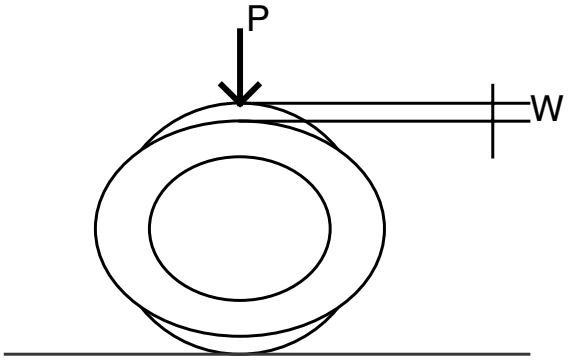

Fig. 4 Radial deformations due to a lateral load on a section of pipe.

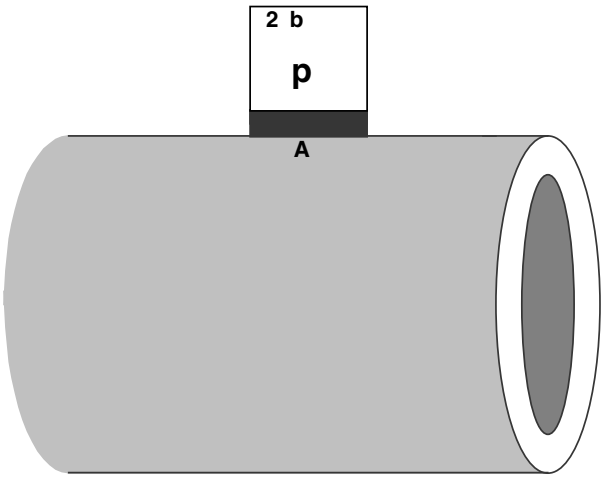

Fig. 5 A concentrated load on a small length of pipe, simulating an indenter under elastic conditions.

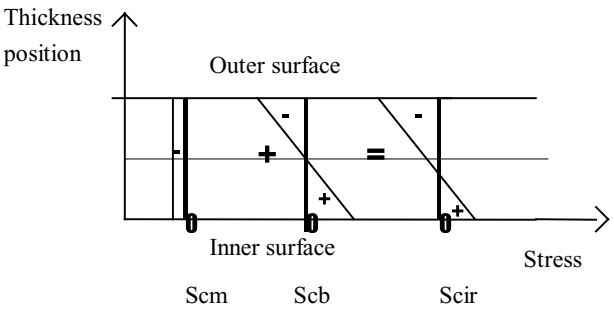

Fig. 6 The circumferential stress state in the pipe of Fig. 5, as the sum of a compressive membrane (S_{cm}) and a bending (S_{cb}) component.

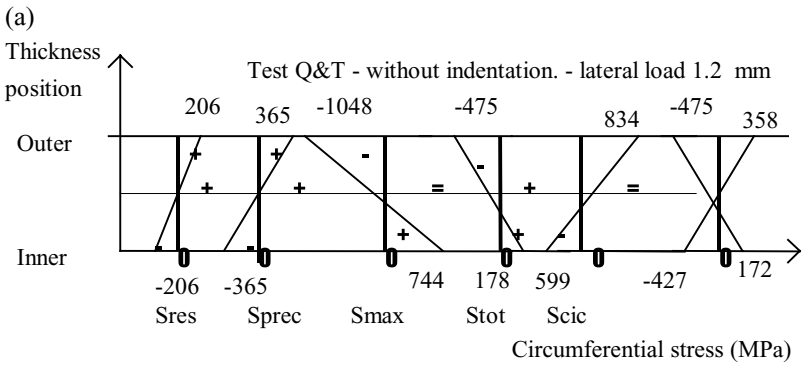

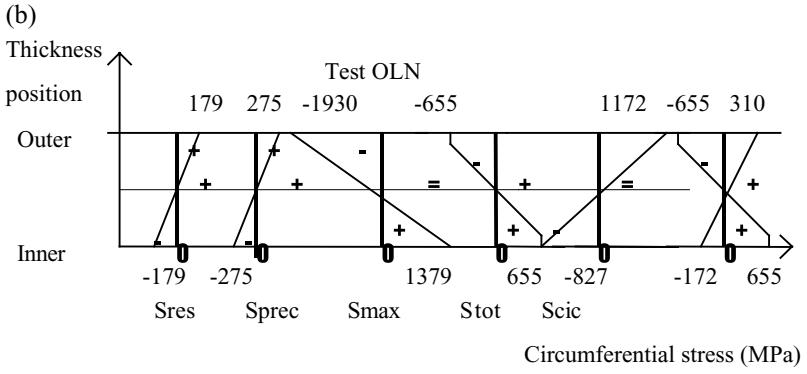

Fig. 7 Stress state in the indent during cyclic loading, when subjected to lateral compression, without previous plastic indenting: (a) material QT, (b) material OLN.

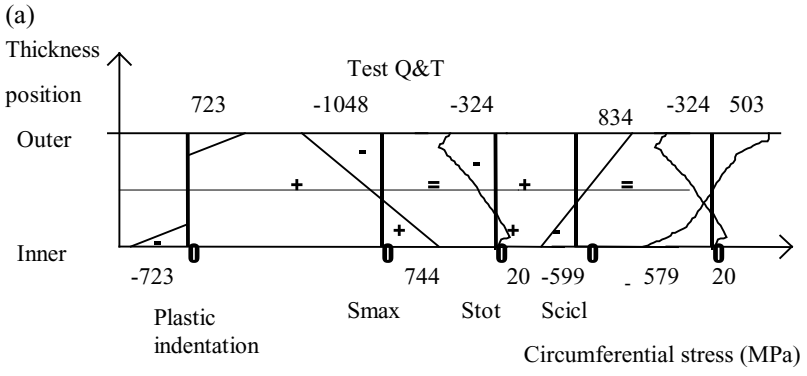

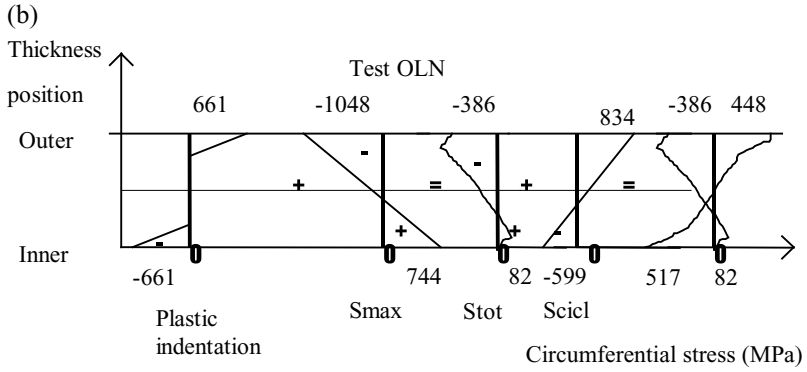

Fig. 8 Stress state in the dent during cyclic loading, when previously subjected to plastic indenting, without lateral compression: (a) material QT, (b) material OLN.

pipe and the neighbouring pipes and the size (length and width) of the protuberance acting as an indenter. With the results of the previous models, the superposition principle can be used in the way schematized in Fig. 7 to assess the stress state during cyclic indentation on a pipe when simultaneously subjected to lateral compression but without previous plastic indentation. Similarly, in Fig. 8 a pipe is represented during a cyclic indentation test that has been previously subjected to plastic indenting without lateral compression.

The stress states defined in the indentation area, as seen in Figs 7 and 8, are

S_{res}: residual manufacturing stress (static),
S_{prec}: stresses caused by lateral compression (static).
S_{max}: stress state when the maximum load is reached for the first time during the cyclic indentation test,
S_{tot}: sum of the three previous stress states. In some cases the maximum stresses exceed the yield strength of the material, and plasticity develops near the surfaces (Fig. 8b),
S_{cicl}: when unloading the first cycle, an elastic relaxation of the stresses takes place. Its value is the cyclic amplitude S_{cicl}. The extreme values of the successive stress states generated during the test after this first cycle are represented in the last part of the figures.

The stress states due to the residual stresses and lateral compression, S_{res} and S_{prec}, are destroyed during the process of local plastic indentation applied before the initiation of the fatigue test. In these tests, the initial plastic deformation eliminates the static stress state and generates a new distribution of plasticity induced residual stresses (Fig. 8). The maximum value of $S_{ind.plast}$ is similar to the yield stress of the material, and is located near the outer (compression) and inner (traction) surfaces, respectively.

FULL-SCALE FATIGUE TESTS

Full-scale experimental testing was designed to reproduce TF cracks, developed from both surfaces of the pipe and both propagated to at least 30% wall thickness. A modified hydraulic 170 ton press was used, pressure gauges and valves were added to control applied cyclic load, which varied between 10 and 20 ton, at a frequency of 1 Hz. Preliminary tests allow the definition of the geometry of the indenters, the load cycles to apply and the instrumentation methods.

Twelve fatigue tests were carried out on 180-mm inner diameter, 9-mm-thick API N80 OLN and QT seamless pipes. Two indenter geometries were used: cylindrical (tests 1 and 2) and flat (tests 3–12). Figure 9 shows a two-flat-indenter test in which cyclic load is applied horizontally and the indents are indicated by white arrows. Lateral compression was applied to the pipes in order to obtain adequate stress triaxiality in the area of the indentation, as defined in the 'Simplified Models of Stress States during Transit Fatigue' section. Two pipes, thicker and of smaller diameter than the pipes being tested, were adjusted to each side of the sample by 30 mm bolts through holes in the sample (Fig. 9).

The load–displacement relationship was monitored during previous plastic indentation of the indents to verify the analytic estimates of applied stresses. Test pipes were instrumented with strain gauges (Fig. 10) around the contact area of the indenters. In this way, it was possible to monitor longitudinal and circumferential strains during the tests in order to detect the initiated cracks.[13] The relationship between instantaneous load and strains was used to verify the values of lateral compression, local variations of rigidity in the areas of both indenters and the stress redistribution in

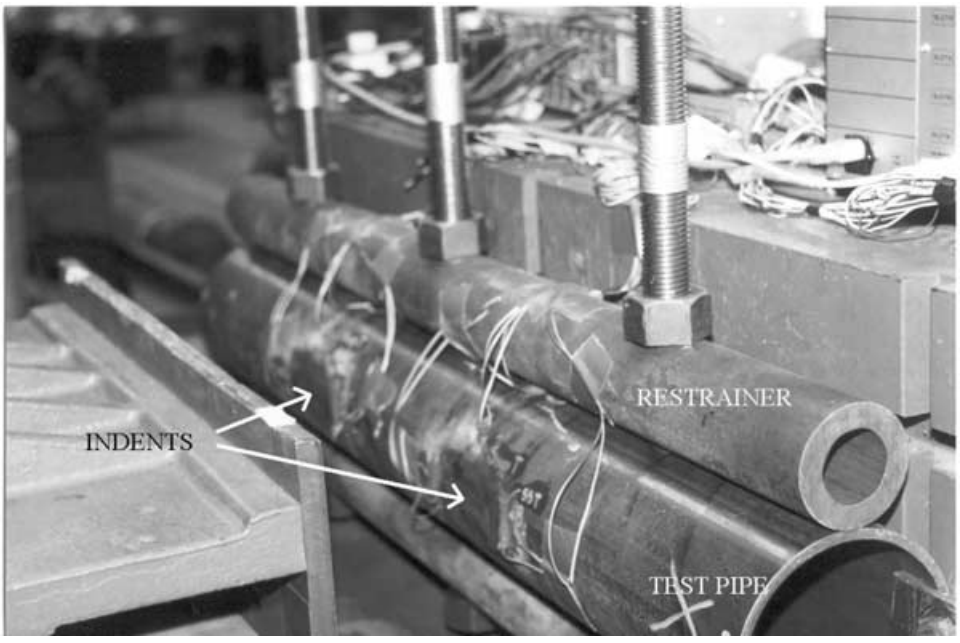

Fig. 9 Full-scale fatigue tests, two thick pipes bolted to each side of the pipe being tested.

Table 2 Experimental data and results of full-scale cyclic indentation fatigue tests

Cyclic load	Test	No	Material	S_{ext} (Mpa)	S_{int} (Mpa)	Total life $\times 10^3$	Propagation % ext/int
19 ton	Cylindrical actuator	2	N			100	
19 ton	Without	3	N	310.3	655	40	25/75
	previous plastic indentation	4	Q and T	448.2	724	40	25/75
9.5 ton	Double indenter	5	N	310.3	655	180	30/70
9.75 ton	With	6	N	448.2	82.7	200	70/30
	previous plastic indentation	7	Q and T	503.3	20.7	90	70/30
9.75 ton	Without	8	N	331	206.8	390	60/40
	previous plastic indentation	9	Q and T	358.5	172.4	–	–
		10	N	413.7	199.9	400	65/35
		11	Q and T	655	165.5	–	–
11.3 ton		12	Q and T	517.1	186.2	320	–

Fig. 10 Strain gauge instrumentation and typical crack developed under cyclic indenter.

the pipe wall as the cracks progressed. Beach marks were introduced in the crack surfaces by means of a periodic reduction of the cyclic load. A boroscope (X20), a travelling microscope (X50) and penetrating dies were also used to monitor crack growth from the outer and inner surfaces.

The results of each test allowed the adjustment of load and restraint conditions for the following tests. Table 2 summarizes the particular conditions of each test, experimental data and results. Figure 7a and b correspond to tests 9 and 5, while Fig. 8a and b correspond to tests 7 and 3, respectively.

Preliminary tests (1 and 2) were carried out with 120-mm-diameter cylindrical indenters, and a lateral compression characterized by an elastic lateral displacement $W = 1$ mm. After 100 000, cycles a series of surface cracks forming an elliptic pattern was obtained, much different from the longitudinal crack looked for. Therefore, the shape of the indenter was changed. Tests 3 and 4 were carried out with a single 75-mm-wide flat indenter, in materials OLN (test 3) and QT (test 4), without previous plastic indentation. Lateral compression was reduced to an elastic displacement $W = 0.9$ mm, equivalent to a $S_{prec} = 275.8$ MPa in the outer surface of the pipe. This S_{prec} is still rather large and would be produced by a 15-m-high pipe stack. The applied cyclic force in the indenter was 19 ton. The total fatigue life was 40 000 cycles for both materials, up to when the cracks propagated through the wall. Multiple non-coplanar cracks initiated, and propagation was predominantly from the inner surface (75% of wall thickness). These results lead to

the conclusion that the load applied by the indenter was excessive.

Test 5 was carried out with two flat 75-mm-wide indenters in OLN material (as indicated in Fig. 9). In this way, information given by each test would double. A previous 1.5-mm-deep plastic indentation was done with two 20-mm-wide indenters, and an artificial 10-mm-long, 1-mm-deep longitudinal notch was machined on the outer surface of one of the indented areas. The cyclic force was 9.5 ton per indenter, and the load ratio (minimum to maximum) was $R = 0.38$. This is a high value, but was necessary to control the minimum load in the test machine. The total fatigue life was 180 000 cycles, up to when the cracks propagated through the thickness. Cracks initiated at the outer surface. The previous plastic indentation promoted a triangular contact area with the indenters during the cyclic test, in a region away from the predeformed area with the artificial defect. At about 100 000 cycles, cracks growing from the outer surface retarded and cracks from the inner surface started to grow.

Tests 6 (OLN) and 7 (QT) were carried out with two 76.2-mm plane indenters. A longitudinal 0.5-mm-deep, 120-mm-long notch was machined on the inner surface of one the areas affected by the indenters. A 1.5-mm-deep previous plastic indentation with the same indenter was introduced in both materials so that the lateral compression was $W = 1.2$ mm. Minimum, maximum and cyclic loads in the indenter were 19110, 95550 and 76440 N, respectively. Total fatigue lives were 200 000 cycles (material N) and 90 000 cycles (material QT). Initiation of cracks was from the outer surface. The notch in the inner surface tended to accelerate and align the cracks initiated in the outer surface, but it did not exercise an important influence on the total fatigue life. The final crack shape was 70% on the outer surface and 30% on the inner surface.

Tests 8 (OLN) and 9 (QT) were carried out with a smaller cyclic load than the previous tests and without previous plastic indentation, but with larger lateral loads. It was expected that larger tensile cyclic stresses would be generated in the inner surface, and therefore cracks would initiate in that region. Two 76.2-mm flat indenters were used and a 0.5-mm-deep, 120-mm-long defect was machined in the inner surface of one of the indented areas. The lateral compression was $W = 0.75$ mm, which is equivalent to the static weight of a 24-m-high column of pipes. Minimum, maximum and cyclic loads in each indenter were 12 250, 61 152, 49 000 N, respectively. The total fatigue life was 390 000 cycles for the OLN material and infinite for the QT material. Initiation of cracks occurred from the outer surface. The inner notch did not have any influence; cracks in both indents grew similarly. The final relationship of the cracks was 60% on the outer surface and 40% on the inner surface.

Results of tests 8 and 9 proved that the lateral compression was insufficient. Tests 10 (OLN) and 11 (QT) were carried out with similar conditions to tests 8 and 9, but with an increased lateral compression $W = 1.2$ mm. Minimum, maximum and cyclic loads in each indenter were 12 250, 61 152, 49 000 N, respectively. Total fatigue lives were 400 000 cycles for the OLN material and infinite for the QT material. Crack initiation still occurred in the outer surface, and the inner notch did not have any influence. The final relationship of cracks was 65% at the outer and 35% at the inner surfaces. It was concluded that more severe cyclic load was necessary. Test 12 (QT) was carried out under similar conditions to test 11, but with a cyclic indentation load of 57 000 N. The total fatigue life was 320 000 cycles.

DISCUSSION OF RESULTS

The full-scale tests succeeded in replicating actual fatigue crack geometries found in pipeline failures related to TF in ships.[8] Cracks initiated first from the outer surface, with the final crack geometry at around 65% on the outer surface and 35% on the inner surface.

It is known that the effective part of the applied cyclic stresses, that is, the stress amplitude directly related to fatigue crack propagation, is the portion of the stress cycle during which the tip of the crack is open. In these conditions, reversed plasticity mechanisms in the material close to the crack tip take place, in ferritic–pearlitic steels these mechanisms eventually lead to the exhaustion of ductility and crack propagation.[15] No crack closure measurements were carried out in this study, so the effective cyclic stress for fatigue crack growth is approximated to the positive part of the applied stress cycle. Then we can define

ΔS = positive part of S_{cicl}, with maxima in both surfaces,
ΔS_{ext} = effective cyclic stress in the outer surface of the pipe,
ΔS_{int} = effective cyclic stress in the inner surface of the pipe.

When indents were subjected to a single plastic indentation previous to fatigue cycling, ΔS_{ext} in the subsequent cycles is larger in the QT material than in the OLN material. This is due to the effect of a larger plasticity-induced residual stress, and is noticeable when comparing the schematic stress models of Figs 7 and 8. When not subjected to previous plastic indentation, ΔS_{ext} is also larger in the QT material than in the OLN material, due to the effect of a larger manufacturing S_{res}. Figures 7 and 8 also show that, under similar conditions, ΔS_{ext} should be larger in tests with previous plastic indentation than in tests without this indentation. For similar values of static stresses, ΔS_{ext} can increase when reducing the cyclic load.

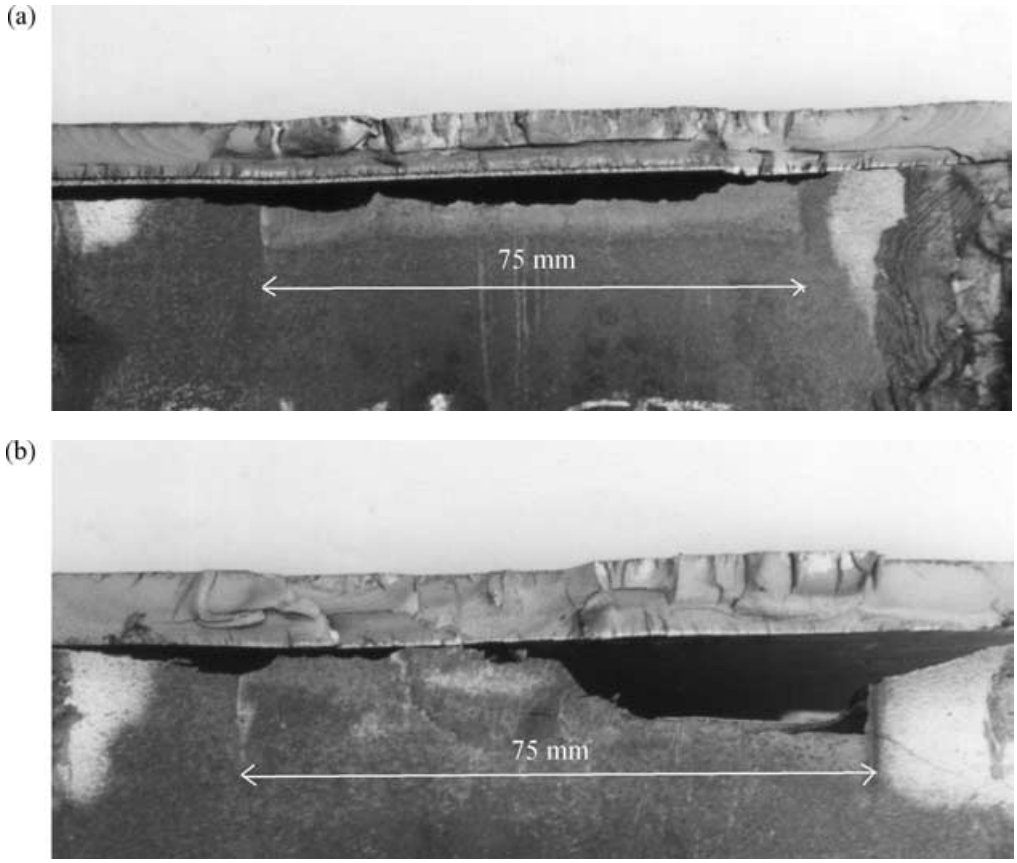

Fig. 11 Fracture surfaces of the two indenters after test 6.

The effective cyclic stress in both the surfaces of the pipe is directly related with crack propagation from both surfaces. In these ferritic–pearlitic steels the growth rate of a fatigue crack is approximately proportional to ΔS^3. Therefore, crack propagation is predominantly from the surface where ΔS is larger. For example, if the outer surface is subjected to ΔS 30% larger than the inner surface, then the initial crack growth rate should be 100% larger from the outer side. The presence of long cracks alters the stress distribution through the wall, modifying the predictions of Figs 7 and 8 as the cracks grow. Earlier crack initiation and faster growth during the early stages of propagation combine in ensuring that in those tests where S_{ext} is larger than S_{int}, cracks from the outer surface are dominant, and vice versa.

Figure 10 shows the outer surface of the fatigue indented area after test 6. The irregular surface path of the developed cracks is characteristic of cracks formed by coalescence of non-coplanar microcracks. Figures 11 and 12 show the cracks developed in the full-scale tests with previous plastic indentation. The position of the 75-mm-wide indenter is indicated in each figure. Fracture surfaces are shown on top, and crack traces on the outer pipe surface are shown on the bottom. Figure 11 corresponds to each of the two indenters after test 6 (OLN), while Fig. 12 corresponds to each of the two indenters after test 7 (QT). The machined notches in the inner surfaces of the pipes and the rather planar fracture surfaces can be seen in Figs 11a and 12a, while a larger mismatch between planes of growing cracks is seen in the cracks at the un-notched indents (Figs 11b & 12b). Other than this, all four samples are similar. In all these tests, multiple cracks initiated first in the outer surface of the pipes, and the relationship of the final crack is very similar in all tests, i.e. of the order of 70% on the outer and 30% on the inner surface.

With respect to the influence of preexisting surface defects, the 0.5-mm-deep notches machined in the inner surfaces of the OLN and QT pipes failed to provide any significant influence in the TF behaviour of the pipes. It is known that seamless pipes can exhibit long shallow defects as a result of the manufacturing process, which would be expected to influence the fatigue live. However, experimental evidence shows that crack initiation from the outer surface of the pipes always occur after a certain degree of plastic deformation due to contact with an indenter, which modifies the majority of any surface discontinuity. In tests 6 and 7 (Table 2), which had two indents

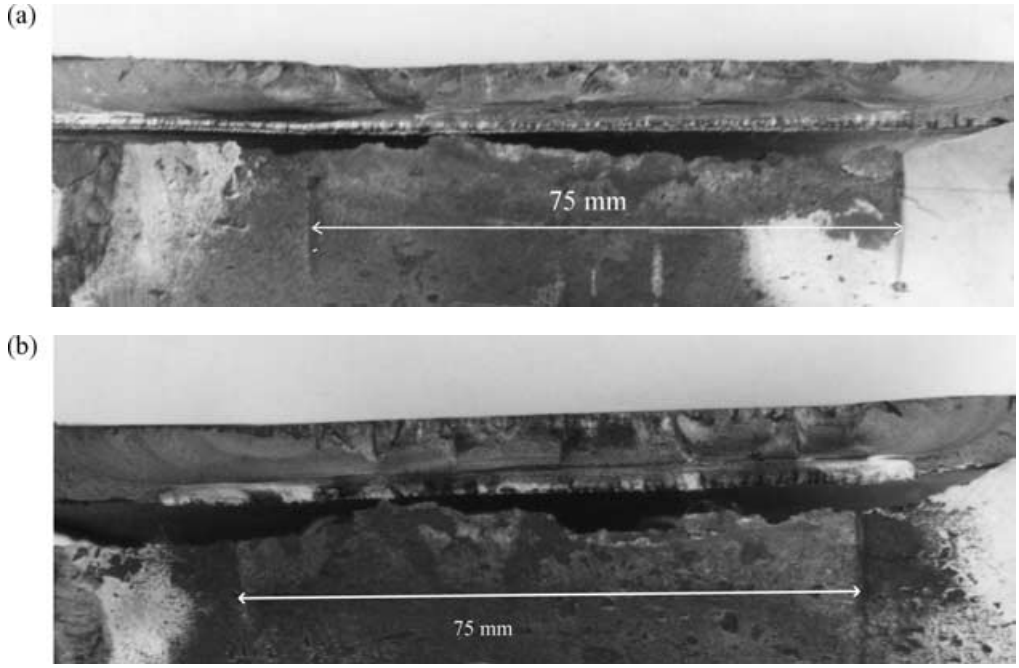

Fig. 12 Fracture surfaces of the two indenters after test 7.

in each pipe, a 0.5-mm-deep longitudinal notch was cut in the inner pipe surface at one of the indents. Interestingly, in both cases the fatigue crack propagation rate was about half at the notched indentations. The reason is that the notches in the inner surfaces constrained the cracks from the inside to grow in that particular plane. Outside the notch stress concentration region the crack fronts were not in the most stressed section.

With respect to the influence of microstructure, the results from the literature on fatigue lives in ferritic–pearlitic steels are usually within the scatter band for the QT steels. In our case, however, microstructural parameters seem to have an appreciable effect on the fatigue crack initiation process. For a given effective cyclic stress amplitude, Fig. 3a and b shows that fatigue initiation lives are 100% longer and propagation rates are 30% lower in the QT steel pipe than in its OLN counterpart. On the other hand, effective (positive) cyclic stress amplitudes in the full-scale fatigue tests with previous plastic indentation are 10% larger in QT steel. For a Paris exponent of 3, these opposed effects are balanced, and microstructure does not have a significant influence in transit crack growth rates. This is not the case in tests without previous plastic indentation, in which the fatigue lives in the OLN pipes were shorter than in QT pipes. However, the fatigue lives were substantially larger in both pipes.

The differences in fatigue crack patterns and lives for tests with and without previous plastic indentation allow us to conclude that the most probable condition for actual TF failures is related to a plastic indentation that occurs sometime during shipping. The most probable sources of indentation are protruding elements at the sides of the cargo bays in ships. The need for lateral compression means that subsequent fatigue crack growth is most probable in the lower pipes of a high pipe stack.

The lateral compression used in tests 6, 7, 10, 11 and 13 was applied with a load equivalent to a height of 40 m of pipes of the same geometry. This is far too high for a pipe stack, but also equivalent to a pile of 20 m subjected to a dynamic acceleration of 2 g, which is attainable during a storm. This weight can also be attained with a much lower pile and less severe wave conditions, if heavier pipes (i.e. thick, low diameter) are placed on the top of less dense, more flexible pipes.

Full-scale test results show that once an indent was produced in the pipe wall, the total fatigue life was between 300 000 and 400 000 cycles (Table 2). Considering a wave period of around 1–10 sec, a total fatigue life of 300 000 cycles can be consumed in a period of 6–40 days. Fatigue cracks could be initiated in less time, and even if not through the thickness they could still lead to failures when the pipe is first subjected to pressure. We see then that the length and conditions of a normal ship journey are enough to justify the occurrence of TF defects in pipes, if not stored properly. This has been recognized by the industry and translated into more stringent requirements, such as those introduced in the 1996 revision of API 5LW 'Recommended Practice for transportation of line pipe on barges and marine vessels'.[16] The results of this study show that some additional precautions could be implemented to

reduce the probability of TF in sea shipment, such as to extreme precautions to prevent plastic indentation of the pipes and to store the heavier or stiffer pipes in the lower part of the pile.

CONCLUSIONS

The mechanical conditions related to TF phenomenon were studied. The model applied to sea shipment OCTG pipes considers the presence of indenters and some special (but really possible) conditions, such as critically high accelerations and a sufficiently large number of cycles to produce TF damage. Fatigue tests were carried out in laboratory samples and in full-scale seamless API 5CT N80 pipes (one QT and the other OLN). Their complex stress states and crack growth patterns were analysed for different conditions of applied load, lateral restraint and previous plastic deformation.

No appreciable differences with pipe strength were observed in fatigue life (initiation as well as propagation) when the pipes were subjected to previous plastic indentation. Although seamless pipes can exhibit different manufacturing defects, longitudinal machined notches in the pipe surfaces did not reduce TF lives. The reasons for this being related to plasticity in the outer surface and non-coplanar crack growth in the inner surface.

It was experimentally demonstrated that TF is more likely when piling up many pipes for transportation, if there is previous plastic indentation followed by cyclic loading in highly restrained conditions. Such cases would typically be triggered when a pipe in the lower part of the cargo slides and hits against a hard protuberance. Further fluctuating loading against the same protuberance allows fatigue crack initiation and growth. To have TF without previous plastic indentation, a higher pile of pipes is required. A sufficient equivalent dynamic load can also be reached, in the case of more flexible pipes, when heavier pipes are stored on top of lighter ones, or when heavy storms increase accelerations on the stored pipes.

Acknowledgements

This work was funded by Consejo Nacional de Investigaciones Científicas y Técnicas (CONICET) and grant PICT 1204586 by Agencia Nacional de Promocion Cientifica, Argentina.

REFERENCES

1 Atterbury, T. J. (1963) Cyclic stresses in rail shipment of pipe. *The Oil & Gas Journal*, *Sept. 13*.
2 Bruno, T. V. (1988) How to prevent transit fatigue to tubular goods. *Pipe Line Industry*.
3 Wang, K. and Smith, E. *The effect of mechanical damage on fracture initiation in line pipe—Part 1: Dents*. CANMET Physical Metallurgy Research Laboratories, report ERP/PMRL 82-11(TR).
4 Hopkins, P., et al (1992) *The resistance of gas transmission pipelines to mechanical damage*. European Pipeline Research Group, Mechanical Damage Working Party, paper VIII-3-17.
5 Elber, R. J., Maxey, W. A., Bent, C. W. and MacClure, G. M. (1981) *The effects of dents on the failure characteristics of line pipe*. Battelle NG18, report 125.
6 Kiefner, J. F. and Maxey, W. A. (1986) Evaluating pipeline integrity. Flaw behaviour during and following high pressure testing. In: *Proceedings of the 7th Symposium on Line Pipe Research*, Houston, paper 15.
7 API RP 579. (2000) *Fitness for Service*. American Petroleum Institute.
8 API 5CT. (2001) *Specification for Casing & Tubing*, 7th edn. American Petroleum Institute.
9 Roark, R. *Formulas for Stress and Displacement*, 5th edn, McGraw-Hill Book Company, p. 496.
10 Fuchs, H. O. (1980) *Metal Fatigue in Engineering*. Wiley Interscience Publication, New York.
11 Broek, D. (1982) *Elementary Engineering Fracture Mechanics*. Kluwer Academic Publishers, Dordrecht, The Netherlands.
12 Tada, H., Paris, P. C. and Irwin, G. R. (1973) *The Stress Analysis of Cracks Handbook*, Del Research Corp., Hellertown, Pennsylvania.
13 Otegui, J. L., Mohaupth, U. H. and Burns, D. J. (1991) A strain gauge technique for monitoring small fatigue cracks in welds. *Eng. Fract. Mech.* **40**, 549–570.
14 Newman, J. and Raju, I. (1981) An empirical stress–intensity factor equation for the surface crack. *Eng. Fract. Mech.* **15**, 185–201.
15 Anderson, T. L. (1995) *Fracture Mechanics, Fundamentals and Applications*, 2nd edn, CRC Press, Miami.
16 API RP 5LW. (1996) *Recommended practice for transportation of line pipe on barges and marine vessels*, 2nd edn, American Petroleum Institute.